JOURNAL OF CHEMICAL & ENGINEERING DATA

ARTICLE

pubs.acs.org/jced

Measurement and Correlation of the Thermal Conductivity of 2,3,3,3-Tetrafluoroprop-1-ene (R1234yf) and *trans*-1,3,3,3-Tetrafluoropropene (R1234ze(E))

Richard A. Perkins* and Marcia L. Huber

Thermophysical Properties Division, National Institute of Standards and Technology, Boulder, Colorado 80305-3337, United States

Supporting Information

ABSTRACT: New experimental data on the thermal conductivity of 2,3,3,3-tetrafluoroprop-1-ene (R1234yf) and *trans*-1,3,3,3-tetrafluoropropene (R1234ze(E)) are reported that allow the development of wide-range correlations. These new experimental data, covering a temperature range of (242 to 344) K for R1234yf and (203 to 344) K for R1234ze(E) at a pressure range of (0.1 to 23) MPa, are used to develop correlations for the thermal conductivity. The experimental data reported here have an uncertainty of less than 1 % for liquid measurements and for gas at pressures above 1 MPa, increasing to 3 % for gas at low pressures (less than 1 MPa). On the basis of the uncertainty of and comparisons with the present data, the thermal-conductivity correlations for R1234yf and R1234ze(E) are estimated to have relative expanded uncertainties of 3 % at a 95 % confidence level.

INTRODUCTION

Concern about the global warming potential (GWP) of common heat-transfer fluids and refrigerants has stimulated research to find replacement fluids with lower GWPs. Recently, unsaturated fluorinated compounds known as hydrofluoro-olefins (HFOs) have been identified as promising fluids due to their extremely short atmospheric lifetime resulting from their reactivity with atmospheric hydroxyl radicals.[1] Two such HFOs are the fluorinated propene isomers 2,3,3,3-tetrafluoroprop-1-ene (R1234yf) and *trans*-1,3,3,3-tetrafluoroprop-1-ene (R1234ze(E)). In this manuscript, extensive measurements are reported for the thermal conductivity of 2,3,3,3-tetrafluoroprop-1-ene (R1234yf) and *trans*-1,3,3,3-tetrafluoroprop-1-ene (R1234ze(E)) in their liquid and vapor phases at temperatures from 242 K (for R1234yf) and 203 K (for R1234ze(E)) to 344 K. On the basis of these accurate experimental data, correlations for the thermal conductivities of both fluids are developed that cover the entire fluid region.

EXPERIMENTAL METHOD

Sample Materials. The supplier's analysis of the sample of R1234yf indicated a purity of 99.96 %. Our own analysis by gas chromatography combined with mass spectrometry and infrared spectrophotometry (carried out according to the protocols of Bruno and Svoronos[2,3]) revealed only very small impurity peaks that were too small to permit identification. The sample was degassed by freezing in liquid nitrogen and evacuating the vapor space. The sample as received contained a considerable amount of dissolved air, and a total of eight freeze−pump−thaw cycles were carried out. On the final pumping cycle the initial pressure in the vapor space was $4 \cdot 10^{-3}$ Pa.

The supplier's analysis of the sample of R1234ze(E) indicated a purity of 99.993 %. Our own analysis by gas chromatography combined with mass spectrometry and infrared spectrophotometry (carried out according to the protocols of Bruno and Svoronos[2,3]) revealed only very small impurity peaks that were too small to permit identification. The sample was degassed by freezing in liquid nitrogen, evacuating the vapor space, and thawing. The pressure over the frozen material on the fourth and final freeze−pump−thaw cycle was $1 \cdot 10^{-4}$ Pa.

Transient Measurements. The measurements of thermal conductivity were obtained with a transient hot-wire instrument that has previously been described in detail.[4] During an experiment, the hot wires functioned as both electrical heat sources and resistance thermometers to measure the temperature rise. The measurement cell consisted of a pair of hot wires of differing length operating in a differential arrangement to eliminate errors due to axial conduction. The fluid around the hot wires was contained in the concentric cylindrical region bounded by the wire and the copper vessel with an inner diameter of 9 mm. The transient hot wires were enclosed by a copper pressure vessel that could be maintained at temperatures from (30 to 345) K with samples in the liquid, vapor, or supercritical gas phases at pressures from near (0 to 70) MPa. Initial cell temperatures, T_i, were determined with a reference platinum resistance thermometer with an uncertainty of $u(T_i) = 0.005$ K, and pressures, P_e, are determined with a pressure transducer with an uncertainty of $u(P_e) = 7$ kPa. The measurements were made with bare platinum hot wires with a diameter of 12.7 μm. All reported uncertainties are for a coverage factor of $k = 2$, approximately a 95 % confidence interval.

The basic theory that describes the operation of the transient hot-wire instrument is given by Healy et al.[5] The hot-wire cell was designed to approximate a transient line source as closely as possible, and deviations from this model are treated as corrections to the experimental temperature rise. The ideal temperature

Special Issue: Kenneth N. Marsh Festschrift

Received: July 28, 2011
Accepted: September 8, 2011
Published: September 26, 2011

rise ΔT_{id} is given by

$$\Delta T_{id} = \frac{q}{4\pi\lambda}\left[\ln(t) + \ln\left(\frac{4a}{r_0{}^2 C}\right)\right] = \Delta T_W + \sum_{i=1}^{10} \delta T_i \quad (1)$$

where q is the power applied per unit length, λ is the thermal conductivity of the fluid, t is the elapsed time, $a = \lambda/(\rho C_p)$ is the thermal diffusivity of the fluid, ρ is the density of the fluid, C_p is the isobaric specific heat capacity of the fluid, r_0 is the radius of the hot wire, $C = 1.781$ is the exponential of Euler's constant, ΔT_w is the measured temperature rise of the wire, and δT_i are corrections[5] to account for deviations from ideal line-source conduction. During the analysis, a line is fit to the linear section, from (0.1 to 1.5) s, of the ΔT_{id} versus $\ln(t)$ data, and the thermal conductivity is obtained from the slope of this line. Both thermal conductivity and thermal diffusivity can be determined with the transient hot-wire technique as shown in eq 1, but only the thermal conductivity results are considered here. The experimental temperature, T_e, associated with the thermal conductivity is the average wire temperature over the period that was fitted to obtain the thermal conductivity.

For gas-phase measurements, two corrections[5−9] must be carefully considered. First, since the thermal diffusivity of the gas is much different from that of the wire, the correction for the wire's finite radius becomes very significant. Second, the thermal diffusivity of the dilute gas varies inversely with the pressure, so it is possible for the transient thermal wave to penetrate to the outer boundary of the gas region during an experiment at low pressures.[5−9] The preferred method to deal with such corrections is to minimize them by proper design. For instance, the correction for finite wire radius can be minimized with wires of extremely small diameter [(4 to 7) μm], and penetration of the thermal wave to the outer boundary can be eliminated by the use of a cell with an outer boundary of large diameter. However, such designs are often not optimal for a general-purpose instrument, where such extremely fine wires may be too fragile, and large outer dimensions may require too much of a scarce sample, particularly in the liquid phase.

The present transient hot-wire wires require careful correction for the wire's finite radius during such dilute-gas measurements. Also, the measurement duration must be selected to minimize the correction for penetration to the outer boundary due to the relatively small diameter of the concentric fluid region around each hot wire. The full heat capacity correction[5] was applied to the present measurements. Experiments were generally limited to 1.5 s, with 250 measurements of temperature rise as a function of elapsed time relative to the onset of wire heating. Fluid convection was normally not a problem for transient experiments that were 1.5 s in duration or less. For a few of the measurements at the lowest pressures, the outer boundary was encountered at elapsed times less than 1.5 s, so the maximum fit period for such experiments was further reduced to minimize the magnitude of this correction.

Thermal radiative heat transfer between media at two different temperatures T_1 and T_2 increases in proportion to absolute temperature cubed, because it is proportional to $(T_1{}^4 - T_2{}^4) \approx T^3(T_1 - T_2)$ for small temperature differences. For simplicity, the thermal radiation correction was treated as if the samples were transparent to IR radiation. This approximation is considered reasonable since the magnitude of the radiation heat transfer was insignificant at the maximum temperature near 344 K.

Steady-State Measurements. At very low pressures, the transient hot-wire system described above can be operated in a steady-state mode, which requires smaller corrections.[10] The working equation for the steady-state mode is based on a different solution of Fourier's law, but the geometry is still that of concentric cylinders. This equation can be solved for the thermal conductivity of the fluid, λ,

$$\lambda = \frac{q \ln\left(\frac{r_2}{r_1}\right)}{2\pi(T_1 - T_2)} \quad (2)$$

where q is the applied power per unit length, r_2 is the internal radius of the outer cylinder, r_1 is the external radius of the inner cylinder (hot wire), and $\Delta T = (T_1 - T_2)$ is the measured temperature difference between the hot wire and its surrounding cavity.

For the concentric-cylinder geometry described above, the total radial heat flow per unit length, q, remains constant and is not a function of the radial position. Assuming that the thermal conductivity is a linear function of temperature, it can be shown[10] that the measured thermal conductivity is given by $\lambda = \lambda_{T_i}(1 + b_\lambda(T_1 + T_2)/2)$. Thus, the measured thermal conductivity corresponds to the value at the mean temperature of the inner and outer cylinders,

$$\bar{T} = (T_1 + T_2)/2 \quad (3)$$

This assumption of linear temperature dependence for the thermal conductivity is valid only for experiments with small temperature differences. The density assigned to the measured thermal conductivity is calculated from an equation of state (EOS) with the temperature from eq 3 and the experimentally measured pressure. An assessment of corrections during steady-state hot-wire measurements is given by Roder et al.[10]

EXPERIMENTAL RESULTS

The results of the transient and steady-state measurements of the thermal conductivities of R1234yf and R1234ze(E) are tabulated in the Supporting Information (SI). Transient experiments were analyzed over the period from (0.1 to 1.5) s. The expanded uncertainty (Type A) of the slope of the corrected transient-temperature-rise data versus $\ln(t)$ over this time range is given in the tables of transient data (SI). This expanded uncertainty ($k = 2$) depends on both temperature-rise noise and systematic deviations from the heat-transfer model of eq 1; it is less than 0.2 % for the transient measurements in the liquid phase and less than 2 % for the transient measurements in the vapor phase. The uncertainty of the reported thermal conductivity is always larger than the uncertainty of the slope of the ΔT_{id} versus $\ln(t)$, which is given as a measure of the reproducibility and internal consistency of each transient measurement. The tables of steady-state data in the SI provide the start time and the end time for evaluation of the temperature rise and the Rayleigh number that characterizes the level of convection during the experiment. The Rayleigh numbers during the steady-state measurements were generally less than 17 000, corresponding to a 1 % correction to the measured thermal conductivity. Measurements are generally reported for five different applied powers at each initial fluid state point to verify the absence of convection during the measurements for both transient and steady-state

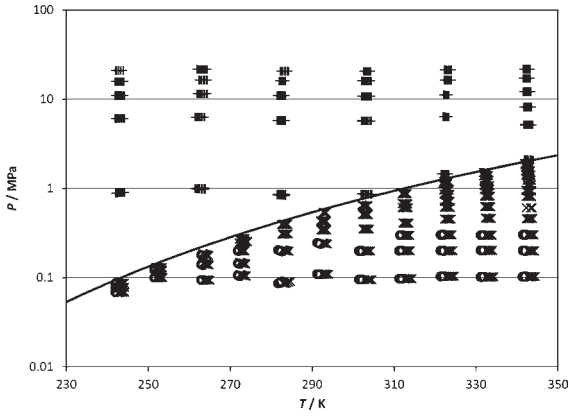

Figure 1. Distribution of the data for the thermal conductivity of R1234yf: ×, transient vapor; ○, steady-state vapor; +, transient liquid. The solid line shows the vapor−liquid saturation boundary.

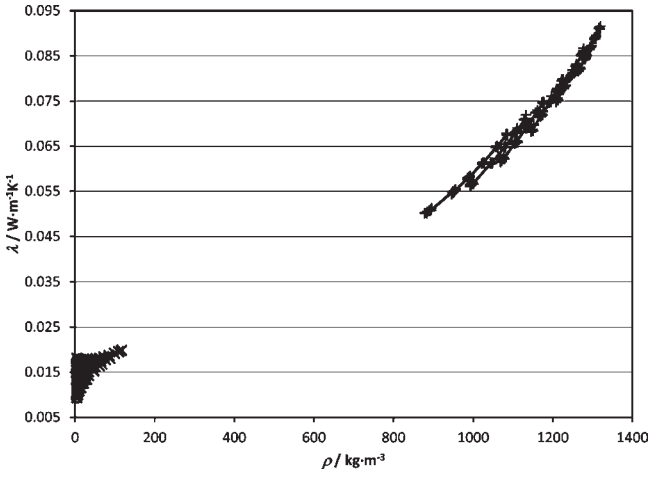

Figure 2. Thermal conductivity of R1234yf as a function of the density calculated at the measured temperature and pressure: ×, transient vapor; ○, steady-state vapor; +, transient liquid; solid lines given by the correlation developed in this work.

measurements. Reported densities, and other fluid property data required for corrections to the measured temperature rise during data analysis, are calculated with short-form Helmholtz equations of state[11,12] for each experimental temperature and pressure associated with the measured thermal conductivity. The uncertainty of the measured initial temperature (ITS-90) is 0.005 K, and the uncertainty of the pressure is 7 kPa. The measured temperature rise and experiment temperature have expanded uncertainties of 0.020 K. The thermal conductivity data have an expanded uncertainty (i.e., a coverage factor $k = 2$, and thus a two-standard-deviation estimate) of 1 % for liquid measurements and for gas at pressures above 1 MPa, increasing to 3 % for gas at low pressures (less than 1 MPa).

R1234yf. The range of state points covered by the present measurements is shown in Figure 1 relative to the vapor-pressure curve of R1234yf. There are 125 steady-state measurements of the vapor phase at temperatures from (242 to 342) K, 354 transient measurements of the vapor phase at temperatures from (242 to 344) K, and 311 transient measurements of the liquid phase at temperatures from (242 to 344) K reported in the SI at pressures up to 23 MPa. These measurements are shown in Figure 2 as a function of calculated density.

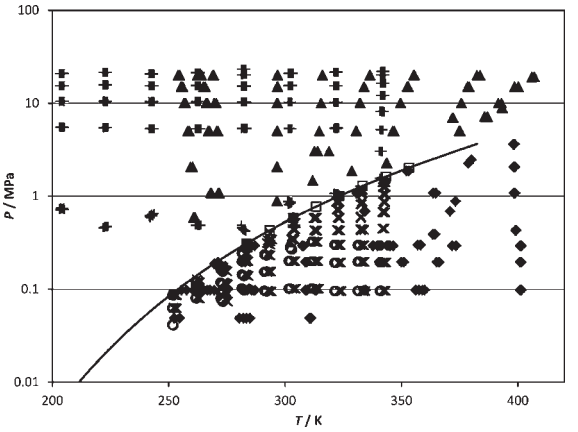

Figure 3. Distribution of the present data for the thermal conductivity of R1234ze(E): ×, transient vapor; ○, steady-state vapor; +, transient liquid. Literature data are shown as: ▲, Grebenkov et al.[13] liquid; ♦, Grebenkov et al.[13] vapor; ●, Miyara et al.[14] saturated liquid; □, Miyara et al.[15] saturated liquid. The solid line shows the vapor−liquid saturation boundary, terminating at the critical point.

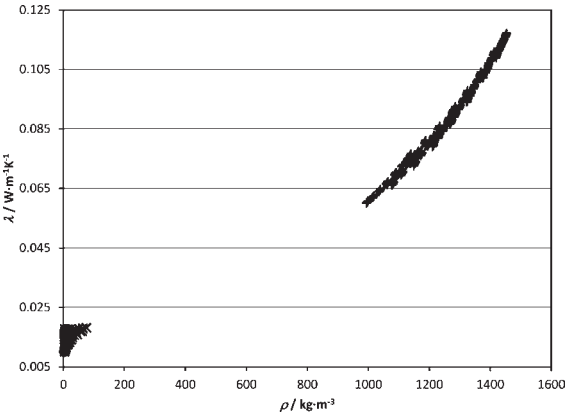

Figure 4. Measured thermal conductivity data for R1234ze(E) as a function of the density calculated at the measured temperature and pressure: ×, transient vapor; ○, steady-state vapor; +, transient liquid; solid lines are given by the correlation developed in this work.

R1234ze(E). The range of state points covered by the present measurements is shown in Figure 3 relative to the vapor-pressure curve of R1234ze(E). Three additional sets of data were found in the literature,[13−15] and these are also shown in Figure 3. There are 152 steady-state measurements of the vapor phase at temperatures from (251 to 342) K, 299 transient measurements of the vapor phase at temperatures from (252 to 343) K, and 452 transient measurements of the liquid phase at temperatures from (202 to 343) K reported in the SI at pressures up to 22 MPa. These measurements are shown in Figure 4 as a function of calculated density.

THERMAL CONDUCTIVITY CORRELATION

We represent the thermal conductivity λ of a pure fluid as a sum of three contributions,

$$\lambda(\rho, T) = \lambda_0(T) + \Delta\lambda_r(\rho, T) + \Delta\lambda_c(\rho, T) \quad (4)$$

where λ_0 is the dilute-gas thermal conductivity, which depends only on temperature, $\Delta\lambda_r$ is the residual thermal conductivity,

and $\Delta\lambda_c$ is the enhancement of the thermal conductivity in the critical region. Both $\Delta\lambda_r$ and $\Delta\lambda_c$ are functions of temperature, T, and density, ρ, with ρ calculated with an EOS for each experimental T and P. In this work, we use recently developed short-form Helmholtz equations of state[11,12] for each fluid; the equations have upper temperature and pressure limits of 410 K and 30 MPa for R1234yf and 420 K and 20 MPa for R1234ze(E). The corresponding density limits for R1234yf and R1234ze(E) are 11.64 mol·L^{-1} and 13.19 mol·L^{-1}, respectively. Some of the thermal conductivity data were measured at temperatures and pressures that exceed these limits, and the extrapolation of the EOS and present thermal conductivity model beyond these limits should be viewed with caution. The critical parameters for R1234yf[12] are T_c = 367.85 K, P_c = 3.3822 MPa, and ρ_c = 475.55 kg·m^{-3}, and for R1234ze(E)[11] they are T_c = 382.52 K, P_c = 3.6363 MPa, and ρ_c = 489.24 kg·m^{-3}.

Dilute-Gas Thermal Conductivity. We represent the dilute-gas thermal conductivity as a polynomial in reduced temperature,

$$\lambda_0(T)/(\mathrm{W\cdot m^{-1}\cdot K^{-1}}) = \sum_{k=0}^{2} A_k (T/T_c)^k \tag{5}$$

with coefficients A_k, where T is the temperature and T_c is the critical temperature.

Residual Thermal Conductivity. We used a polynomial in temperature and density to represent the background, or residual, contribution to the thermal conductivity,

$$\Delta\lambda_r(\rho,T)/(\mathrm{W\cdot m^{-1}\cdot K^{-1}}) = \sum_{i=1}^{5}\left(B_{i,1} + B_{i,2}\left(\frac{T}{T_c}\right)\right)\left(\frac{\rho}{\rho_c}\right)^i \tag{6}$$

with coefficients $B_{i,j}$, where ρ is the density and ρ_c is the critical density. This form has been shown to be adequate to accurately represent other fluorinated refrigerants such as R134a[16] and R125.[17]

Critical Enhancement. Olchowy and Sengers[18] developed a theoretically based, but complex, model for the thermal conductivity enhancement in the critical region. We use a simplified version of their crossover model,[19]

$$\Delta\lambda_c(T,\rho)/(\mathrm{W\cdot m^{-1}\cdot K^{-1}}) = \frac{\rho C_p R_0 k_B T}{6\pi\eta\xi}(\Omega - \Omega_0) \tag{7}$$

where the heat capacity at constant pressure, $C_p(T,\rho)$, is obtained from the EOS, k_B is Boltzmann's constant, R_0 = 1.03 is a universal constant,[20] and the viscosity, $\eta(T,\rho)$, is obtained from an extended-corresponding-states estimation method,[21] as implemented in the National Institute of Standards and Technology (NIST) database REFPROP.[22]

The crossover functions Ω and Ω_0 are determined by

$$\Omega = \frac{2}{\pi}\left[\left(\frac{C_p - C_V}{C_p}\right)\arctan(q_d\xi) + \frac{C_V}{C_p}(q_d\xi)\right] \tag{8}$$

$$\Omega_0 = \frac{2}{\pi}\left[1 - \exp\left(\frac{-1}{(q_d\xi)^{-1} + \frac{1}{3}((q_d\xi)\rho_c/\rho)^2}\right)\right] \tag{9}$$

The heat capacity at constant volume, $C_V(T,\rho)$, is obtained from the EOS, and the correlation length ξ is given by

$$\xi = \xi_0\left[\frac{P_c\rho}{\Gamma{\rho_c}^2}\right]^{\nu/\gamma}\left[\left.\frac{\partial\rho(T,\rho)}{\partial P}\right|_T - \left(\frac{T_R}{T}\right)\left.\frac{\partial\rho(T_R,\rho)}{\partial P}\right|_T\right]^{\nu/\gamma} \tag{10}$$

where the critical amplitudes Γ and ξ_0 are system-dependent and are determined by the asymptotic behavior of the EOS in the critical region. The partial derivative $\partial\rho/\partial P|_T$ is evaluated with the EOS at the system temperature T and at a reference temperature, T_R. For the reference temperature, we select a value where the critical enhancement is assumed to be negligible: $T_R = 1.5T_c$. The exponents γ = 1.239 and ν = 0.63 are universal constants.[19] We have chosen to use values of the critical amplitudes that we consider reasonable for this family of fluids,[17] Γ = 0.0496 and $\xi_0 = 1.94\cdot10^{-10}$ m. The only parameter left to be determined is the cutoff wavenumber q_d (or, alternatively, its inverse, ${q_d}^{-1}$). This parameter can be obtained by regression of data in the critical region; because we do not have data in this region, we used the same value of ${q_d}^{-1}$ of 0.5835 nm that was obtained for R125.[17]

CORRELATION RESULTS

To obtain the coefficients for the thermal conductivity of the dilute gas in the limit of zero density, eq 5, one can extrapolate the thermal conductivity at constant temperature to zero density, provided there are data over a sufficient range of density along an isotherm. An alternative method is to simultaneously fit the dilute-gas thermal conductivity, the excess contribution, and the critical enhancement, eqs 4 to 10, to obtain the dilute-gas coefficients A_k, and the excess coefficients B_{ij}. We chose the latter method, with equilibrium properties from the equations of state.[11,12] We used the fitting program ODRPACK[23] to fit the experimental data obtained in this work to determine the coefficients in eqs 5 and 6, given in Table 1. In addition, to provide a realistic extrapolation behavior of the correlation at very high temperatures (to 1000 K), we included in the regression some estimated dilute-gas values (λ_0) generated from the method of Chung.[24] The state conditions of some of the data points exceeded the limits of the EOS; their results are still included in the statistical analysis, but we recommend caution when extrapolating outside the limits of the EOS. Table 2 provides values of the thermal conductivity calculated for each fluid to allow verification of computer coding of the correlations.

R1234yf Deviations. The present study, comprising 790 points in the liquid and vapor regions from T = (242 to 344) K at pressures up to 22 MPa, is the only data set available for R1234yf. Figure 5 shows deviations between the data and the correlation as a function of density, which was calculated from the measured temperature and pressure with the EOS.[12] Figure 6 shows deviations between the data and the correlation as a function of measured temperature. The correlation accurately represents the present data over the temperature range from T = (240 to 340) K for the liquid and vapor phases at pressures up to 22 MPa. The liquid-phase points are represented to within 1 %, while the vapor-phase points are represented to within 3 %, both at a 95 % confidence level.

R1234ze(E) Deviations. In addition to the present study, comprising 903 points in the liquid and vapor regions at pressures up to 23 MPa, there are three other sets of data in

the literature.[13−15] Grebenkov et al.[13] reported measurements of the liquid and gas phase from T = (252 to 407) K at pressures to 20 MPa that were obtained with a relative steady-state method of coaxial cylinders along isobars. Miyara et al.[14] reported preliminary measurements for mixtures of R1234ze(E) with R32 and gave results for three points for the pure fluid R1234ze(E) in the liquid phase obtained with a transient hot-wire method. More recently, Miyara et al.[15] remeasured the saturated liquid thermal conductivity of R1234ze(E) from (283 to 353) K with an improved transient hot-wire apparatus. These sets were not used in the regression to obtain the coefficients of the correlation and are used for comparison only. Figure 7 shows deviations between the present data and the correlation as a function of density, which was calculated from the measured temperature and pressure with the EOS.[11] The liquid-phase points are represented to within 1 %, while the vapor-phase points are represented to within 3 %, both at a 95 % confidence level. Figure 8 shows deviations between the present data and the correlation as a function of measured temperature, and Figure 9 displays deviations as a function of temperature for all data. The liquid-phase data of Grebenkov et al.[13] are systematically about 25 % lower than our data. The vapor-phase data of Grebenkov et al.[13] are in good agreement with our data at temperatures below 300 K, but as the temperature increases above that, the Grebenkov data begin to increasingly show negative deviations, as seen in Figure 9. The earliest data of Miyara et al. are liquid phase and show positive deviations on the order of 10 % to 20 %. However, the most recent measurements of Miyara et al.,[15] obtained with the

Table 1. Parameters for the Dilute-Gas and Residual Thermal Conductivity of Equations 5 and 6

fluid		R1234yf	R1234ze(E)
Dilute-Gas Thermal Conductivity of eq 5			
k		A_k/(W·m^{-1}·K^{-1})	A_k/(W·m^{-1}·K^{-1})
0		−0.0102778	−0.0103589
1		0.0291098	0.0308929
2		0.000860643	0.000230348
Residual Thermal Conductivity of eq 6			
i	j	B_{ij}/(W·m^{-1}·K^{-1})	B_{ij}/(W·m^{-1}·K^{-1})
1	1	−0.0368219	−0.0428296
1	2	0.0397166	0.0434288
2	1	0.0883226	0.0927099
2	2	−0.0772390	−0.0605844
3	1	−0.0705909	−0.0702107
3	2	0.0664707	0.0440187
4	1	0.0259026	0.0249708
4	2	−0.0249071	−0.0155082
5	1	−0.00322950	−0.00301838
5	2	0.00336228	0.00210190

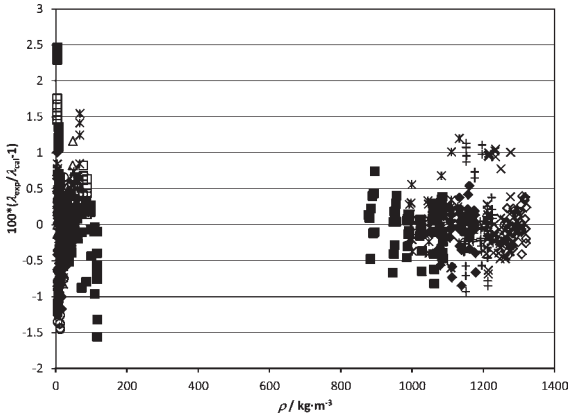

Figure 5. Relative deviation between the present experimental data (transient technique) and the correlation for the thermal conductivity of R1234yf as a function of density. Temperatures shown as: ◇, 243 K; ▲, 252 K; ×, 262 K; ●, 273 K; +, 283 K; ○, 293 K; ◆, 303 K; △, 323 K; ∗, 323 K; □, 332 K; ■, 343 K.

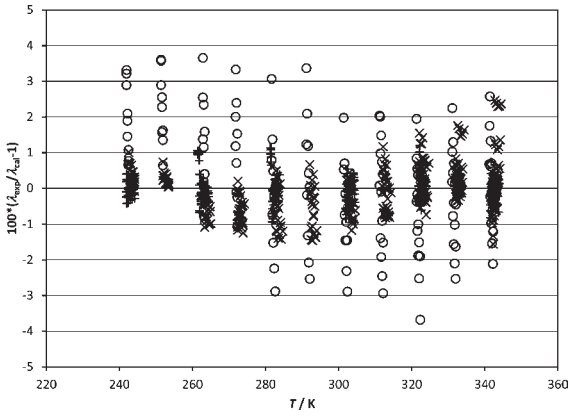

Figure 6. Relative deviation between the present experimental data and the correlation for the thermal conductivity of R1234yf as a function of temperature: ×, transient vapor; ○, steady-state vapor; +, transient liquid.

Table 2. Values of Thermal Conductivity Calculated with the Correlation (Equations 4 to 10) at Specified T and ρ, with the Coefficients in Table 1[a]

		R1234yf		R1234ze(E)	
T	P[b]	ρ	λ	ρ	λ
K	MPa	kg·m^{-3}	W·m^{-1}·K^{-1}	kg·m^{-3}	W·m^{-1}·K^{-1}
250.00	0.050	2.80006	0.0098481	2.80451	0.0098503
300.00	0.100	4.671556	0.013996	4.67948	0.013933
250.00	20.000	1299.50	0.088574	1349.37	0.10066
300.00	20.000	1182.05	0.075245	1233.82	0.085389

[a] The expanded relative uncertainty (k = 2) in the calculated thermal conductivity is 3 %. [b] Pressures calculated with the EOS in refs 11 and 12.

dx.doi.org/10.1021/je200811n |J. Chem. Eng. Data 2011, 56, 4868–4874

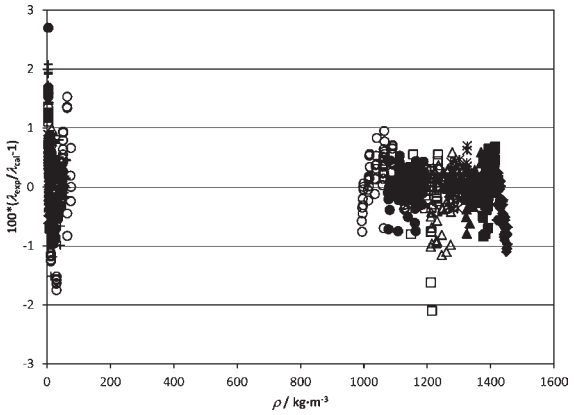

Figure 7. Relative deviation between the present experimental data (transient technique) and the correlation for the thermal conductivity of R1234ze(E) as a function of density, this work. Temperatures shown as: ◆, 203 K; ■, 222 K; ▲, 242 K; ×, 253 K; ∗, 262 K; ◇, 273 K; △, 282 K; -, 293 K; □, 302 K; −, 312 K; ●, 322 K; +, 333 K; ○, 342 K.

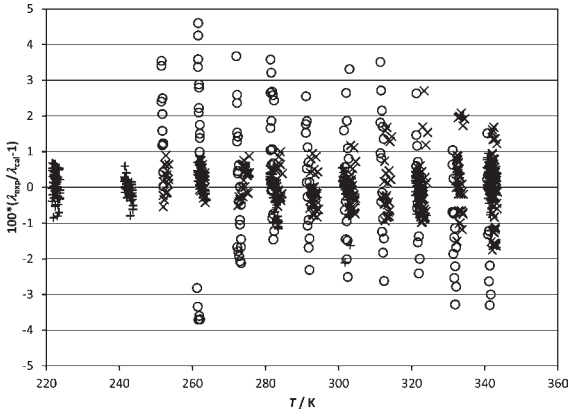

Figure 8. Relative deviation between the present experimental data and the correlation for the thermal conductivity of R1234ze(E) as a function of temperature, this work: ×, transient vapor; ○, steady-state vapor; +, transient liquid.

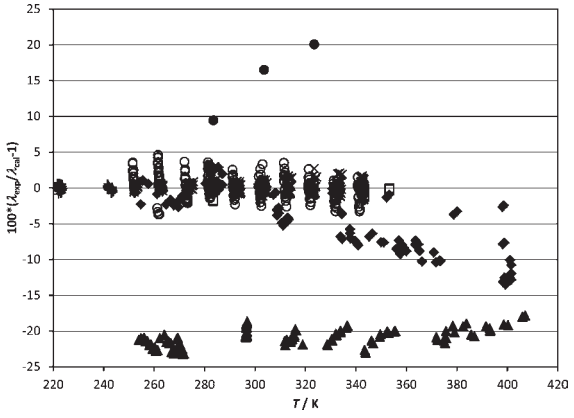

Figure 9. Relative deviation between the experimental data and the correlation for the thermal conductivity of R1234ze(E) as a function of temperature. Present measurements shown as: ×, transient vapor; ○, steady-state vapor; +, transient liquid. Literature measurements shown as: ▲, Grebenkov et al.[13] liquid; ◆, Grebenkov et al.[13] vapor; ●, Miyara et al.[14] saturated liquid; □, Miyara et al.[15] saturated liquid.

transient hot-wire apparatus after improvements that reduced noise, show excellent agreement with our results. The correlation represents the present data in the liquid phase over the temperature range from T = (203 to 343) K at pressures to 23 MPa to within 1 %. The vapor-phase data from (252 to 344) K agree with the correlation to within ± 3 % at a 95 % confidence level. It is expected that the correlation has significantly larger uncertainties at temperatures and densities that are close to the critical point.

CONCLUSIONS

A total of 790 points are reported for the thermal conductivity of R1234yf in the liquid and vapor regions at pressures to 22 MPa. A total of 903 points are reported for the thermal conductivity of R1234ze(E) in the liquid and vapor regions at pressures to 23 MPa. The thermal conductivity data for these fluids have an expanded relative uncertainty of 1 % for measurements removed from the critical point and for gas at pressures above 1 MPa, increasing to 3 % for gas at low pressures (less than 1 MPa) at a 95 % confidence level.

On the basis of these measurements, correlations are developed for the thermal conductivity of R1234yf and R1234ze(E). We could not locate any other data for R1234yf, and only three data sets[13−15] were found for R1234ze(E). Two data sets for R1234ze(E) show significant deviations from the measurements in the present work and from each other, but the most recent data of Miyara et al.[15] show excellent agreement with our measurements. The correlations require thermodynamic property information that was obtained from newly developed equations of state.[11,12] The correlations account for the critical enhancement with a crossover model with a cutoff wavenumber estimated from data for R125, since there are no critical-region data for R1234yf or R1234ze(E). The correlation for R1234yf agrees with the present liquid-phase data to within 1 %, while the vapor-phase data are represented to within 3 % at 95 % confidence levels. The correlation for R1234ze(E) agrees with the present liquid-phase data to within 1 %, while the vapor-phase data agree to within 3 % at 95 % confidence levels. The expanded relative uncertainies (k = 2) for the thermal conductivity calculated for both R1234ze(E) and R1234yf as functions of temperature and density are 3 %. The correlation is expected to have increased the uncertainty in the region near the critical point and at temperatures and pressures beyond the range of the underlying EOS.

ASSOCIATED CONTENT

Supporting Information. Tabulated experimental values (47 pages). This material is available free of charge via the Internet at http://pubs.acs.org.

AUTHOR INFORMATION

Corresponding Author
*E-mail: richard.perkins@nist.gov.

ACKNOWLEDGMENT

We thank Ryan Hulse and Rajiv Singh of Honeywell International for providing the high-purity samples of R1234yf and R1234ze(E). We thank Tara Lovestead of NIST for the chemical analysis of these samples. We also thank Dr. A. Miyara of Saga University (Japan) for sharing preliminary experimental results on

R1234ze(E). We are grateful to the JCED Editors for organizing the "Kenneth N. Marsh Festschrift" and are honored to contribute this manuscript. Above all we wish to express our appreciation to Ken Marsh for many collegial discussions, scientific collaborations, and most of all, for a valued friendship now spanning many years. We extend our warmest wishes to Ken for his retirement and wish Ken and his family all the best in their future endeavors.

REFERENCES

(1) Papadimitriou, V. C.; Talukdar, R. K.; Portmann, R. W.; Ravishankara, A. R.; Burkholder, J. B. $CF_3CF=CH_2$ and (Z)-$CF_3CF=CHF$: temperature dependent OH rate coefficients and global warming potentials. *Phys. Chem. Chem. Phys.* **2008**, *10*, 808–820.

(2) Bruno, T. J.; Svoronos, P. D. N. *CRC Handbook of Basic Tables for Chemical Analysis*, 3rd rd.; Taylor and Francis, CRC Press: Boca Raton, FL, 2011.

(3) Bruno, T. J.; Svoronos, P. D. N. *CRC Handbook of Fundamental Spectroscopic Correlation Charts*; Taylor and Francis, CRC Press: Boca Raton, FL, 2005.

(4) Roder, H. M. A Transient Hot Wire Thermal Conductivity Apparatus for Fluids. *J. Res. Natl. Bur. Stand.* **1981**, *86*, 457–493.

(5) Healy, J.; DeGroot, J. J.; Kestin, J. The Theory of the Transient Hot-Wire Method for Measuring the Thermal Conductivity. *Physica* **1976**, *C82*, 392–408.

(6) Assael, M. J.; Karagiannidis, L.; Richardson, S. M.; Wakeham, W. A. Compression Work using the Transient Hot-Wire Method. *Int. J. Thermophys.* **1992**, *13*, 223–235.

(7) Taxis, B.; Stephan, K. The Measurement of the Thermal Conductivity of Gases at Low Density by the Transient Hot-Wire Technique. *High Temp. High Pressures* **1994**, *15*, 141–153.

(8) Li, S. F. Y.; Papadaki, M.; Wakeham, W. A. The Measurement of the Thermal Conductivity of Gases at Low Density by the Transient Hot-Wire Technique. *High Temp. High Pressures* **1993**, *25*, 451–458.

(9) Li, S. F. Y.; Papadaki, M.; Wakeham, W. A. Thermal Conductivity of Low-Density Polyatomic Gases. In *Thermal Conductivity 22*; Tong, T. W., Ed.; Technomic Publishing: Lancaster, PA, 1994; pp 531−542.

(10) Roder, H. M.; Perkins, R. A.; Laesecke, A.; Nieto de Castro, C. A. Absolute steady-state thermal conductivity measurements by use of a transient hot-wire system. *J. Res. Natl. Inst. Stand. Technol.* **2000**, *105*, 221–253.

(11) McLinden, M. O.; Thol, M.; Lemmon, E. W. Thermodynamic Properties of trans-1,3,3,3-Tetrafluoropropene [R1234ze(E)]: Measurements of Density and Vapor Pressure and a Comprehensive Equation of State (Paper 2189). In *International Refrigeration and Air Conditioning Conference*, 12−15 July, Purdue University, Indiana, United States, 2010.

(12) Richter, M.; McLinden, M. O.; Lemmon, E. W. Thermodynamic Properties of 2,3,3,3-Tetrafluoroprop-1-ene (R1234yf): p-rho-T Measurements and an Equation of State. *J. Chem. Eng. Data* **2011**, *56*, 3254–3264.

(13) Grebenkov, A. J.; Hulse, R.; Pham, H.; Singh, R. Physical Properties and Equation of State for Trans-1,3,3,3-Tetrafluoropropene (Paper 191). In *3rd IIR Conference on Thermophysical Properties and Transfer Processes of Refrigerants*, Boulder, CO, June 23−26, 2009.

(14) Miyara, A.; Tsubaki, K.; Sato, N. Thermal Conductivity of HFO-1234ze(E) + HFC-32 Mixture. In *2010 International Symposium on Next-Generation Air Conditioning and Refrigeration Technology*, Tokyo, Japan, February 17−19, 2010.

(15) Miyara, A.; Tsubaki, K.; Sato, N.; Fukuda, R. Thermal conductivity of saturated liquid HFO-1234ze(E) and HFO-1234ze(E) + HFC-32 mixture. In *23rd IIR International Congress of Refrigeration*, Prague, Czech Republic, 2011.

(16) Perkins, R. A.; Laesecke, A.; Howley, J.; Ramires, M. L. V.; Gurova, A. N.; Cusco, L. *Experimental Thermal Conductivity Values for the IUPAC Round-robin Sample of 1,1,1,2-Tetrafluoroethane (R134a)*; National Institute of Standards and Technology NISTIR 6605: Gaithersburg, MD, 2000; p 150.

(17) Perkins, R. A.; Huber, M. L. Measurement and correlation of the thermal conductivity of pentafluoroethane (R125) from 190 to 512 K at pressures to 70 MPa. *J. Chem. Eng. Data* **2006**, *51*, 898–904.

(18) Olchowy, G. A.; Sengers, J. V. Crossover from Regular to Singular Behavior of the Transport Properties of Fluids in the Critical Region. *Phys. Rev. Lett.* **1988**, *61*, 15–18.

(19) Olchowy, G. A.; Sengers, J. V. A Simplified Representation for the Thermal Conductivity of Fluids in the Critical Region. *Int. J. Thermophys.* **1989**, *10*, 417–426.

(20) Krauss, R.; Weiss, V. C.; Edison, T. A.; Sengers, J. V.; Stephan, K. Transport Properties of 1,1-Difluoroethane (R152a). *Int. J. Thermophys.* **1996**, *17*, 731–757.

(21) Huber, M. L.; Ely, J. F. A Predictive Extended Corresponding States Model for Pure and Mixed Refrigerants Including an Equation of State for R134a. *Int. J. Refrig.* **1994**, *17*, 18–31.

(22) Lemmon, E. W.; Huber, M. L.; McLinden, M. O. *NIST Standard Reference Database 23, NIST Reference Fluid Thermodynamic and Transport Properties Database (REFPROP)*, Version 9.0, Standard Reference Data; National Institute of Standards and Technology: Gaithersburg, MD, 2010.

(23) Boggs, P. T.; Byrd, R. H.; Rogers, J. E.; Schnabel, R. B. *ODRPACK, Software for Orthogonal Distance Regression*; NISTIR 4834; National Institute of Standards and Technology: Gaithersburg, MD, 1992.

(24) Chung, T. H.; Ajlan, L.; Lee, L. L.; Starling, K. E. Generalized multiparameter correlation for nonpolar and polar fluid transport properties. *Ind. Eng. Chem. Res.* **1988**, *27*, 671–679.